18TH WORLD CONFERENCE ON EARTHQUAKE ENGINEERING
WCEE2024
MILAN

MILAN, ITALY
30TH JUNE - 5TH JULY 2024
www.wcee2024.it

SEISMIC PERFORMANCE OF A STICK-BUILT CURTAIN WALL SYSTEM IN A FULL-SCALE BUILDING SHAKE TABLE TEST

S.L. Wynn[1], K.L. Ryan[1], W. Roser[1], Y. Ji[1], T.C. Hutchinson[2] & R. Madeley[3]

[1] University of Nevada, Reno, Reno, USA, sirlathanw@nevada.unr.edu

[2] University of California, San Diego, La Jolla, USA

[3] Technical Glass Products, Snoqualmie, USA

Abstract: *The NHERI TallWood project is at the forefront of research in seismic resilience of tall mass timber buildings. To this end, a full-scale 10-story mass timber building has been subjected to 88 ground motions at the NHERI@UC San Diego outdoor shake table facility to validate self-centering mass timber rocking walls as a seismically resilient lateral force-resisting system (LFRS). The resilience design objectives for the structure were: no damage during design level shaking and minimal damage during risk-targeted maximum considered earthquake (MCE_R) motions. The design of the tall timber test specimen not only considers the seismic resilience of the structural system, but also accounts for the resilience of non-structural components featured in the structure, which include: three cold-formed steel (CFS) framed exterior walls, CFS framed interior partition walls, a modular stair system, and a fire-rated stick-built curtain wall system.*

This paper evaluates the seismic performance of the two-story non-structural curtain wall system. The 60-minute fire-rated curtain wall system features stiff, fire-resistant steel mullions along with 27 mm thick multilayer-laminated glazing. This C-shaped curtain wall system was supported on a steel ledger protruding from the edge of a concrete slab at the base and was attached to the structure at each floor slab. The subassembly has been designed to rack along with the movement of the floor diaphragms, while the glass lites are intended to rotate within the glazing pocket to accommodate movement within the framing. The cantilevered slab supporting the curtain wall caused vertical acceleration amplitudes up to 3 times higher than the input ground motions, which may have caused damage to the door latch mechanism. The results also showed that out-of-plane motions can lead to higher component acceleration amplitudes compared to the in-plane component amplification. After the 88 ground motions, including four MCE_R motions, minimal damage was observed in the curtain wall system and no breakage of the glazing occurred. However, glass movement increased with increasing drift, and the larger drifts led to significant residual displacements.

1. Introduction

In recent years, there has been a growing interest in utilizing mass timber as a structural material in the United States. Mass timber provides several advantages such as faster construction time, lesser demands on the building foundation, and is more environmentally friendly (Pei et al., 2019). As the demand for tall residential and multi-purpose buildings rises due to urban densification, mass timber usage has not been as prominent as steel or concrete in seismic applications due to its limited strength and ductility (Pei et al., 2019). This project, known as the NHERI Tallwood project, aimed to achieve resiliency in the seismic performance of a full-scale 10-story mass timber test specimen by conducting a series of shake table tests on the test specimen.

The resilience objectives were for the structure to remain damage-free or experience minimal damage such that the building is able to quickly recover its functionality after an earthquake.

A building's functionality is not only limited to its structural integrity. Resilience also considers factors such as: whether the building envelope is still functional, if occupants may safely egress, and if the occupancy spaces are still intact. Therefore, nonstructural components have been incorporated throughout the test specimen as well. This paper focuses on the seismic performance of a 2-story, fire-rated stick-built glass curtain wall system, which served as one of four exterior façade subassemblies on the test specimen.

Studies on the seismic performance of curtain wall systems have been mostly limited to component level, in-plane investigations (Behr, 1998; Memari et al., 2011). The method Behr (1998) utilized was adopted by the American Architectural Manufacturers Association (AAMA) in AAMA 501.6 (2018) as the standard test procedure for serviceability and glass fallout resistance for the design of glass curtain walls. However, Behr et al. (1995) found that coupling in- and out-of-plane loading led to increased glass breakage and fallout for susceptible glass types.

This research aims to evaluate the performance of the curtain wall system in the context of resilience objectives and to better understand the mechanisms by which the curtain wall system accommodates movement under 3D motions. This investigation serves as the first of its kind—a curtain wall system attached to a full-scale mass timber building in a shake table test. The curtain wall system in this test program, however, is a fire-rated specialty product that has not undergone component-level seismic testing and does not necessarily represent the seismic performance of all curtain wall products.

2. 10-Story Test Structure and Program

2.1. Specimen Overview

This test program took place at the NHERI@UC San Diego large-scale shake table facility. The main objective was to evaluate the resilience of a 10-story mass timber building utilizing post-tensioned mass timber rocking walls as the lateral force resisting system (LFRS). The 10-story test specimen shown in Figure 1(a) served as the world's tallest full-scale mass timber building ever tested and was constructed using a variety of mass timber products for the floor diaphragms, rocking walls, and gravity frame components. The overall footprint of the test specimen was approximately 10.5 m by 10.5 m (34'x34') and the total height of the building was 34 m tall (112'). The first story was 3.96 m (13') high, while the other 9 stories were 3.35 m (11') high.

The gravity system consisted of laminated veneered lumber beams and columns, and floor diaphragms made up of several types of mass timber products: cross-laminated timber (CLT), veneer-laminated timber, glu-laminated timber, nail-laminated timber, and dowel-laminated timber. The building's LFRS system consisted of two pairs of mass timber rocking walls each in the north-south and east-west directions. The walls in the north-south direction were composed of mass panel plywood (MPP) panels, while the walls in the east-west direction were composed of CLT panels. The rocking walls were equipped with U-shaped flexural plates (UFPs) and post-tensioned (PT) rods. The UFPs served as the main energy dissipation device for the building, which were shown to perform well in the 2-story test performed by Ganey et al. (2017). The PT rods were meant to re-center the rocking wall after lateral movements. Additional details regarding the structural design of the test specimen can be found in Busch (2023).

As mentioned, besides the curtain wall subassembly, the test specimen incorporated a variety of nonstructural components that are critical to the building's functionality including: (1) three exterior cold-formed steel (CFS) framed wall subassemblies, (2) interior CFS-framed walls, and (3) a modular stair system. The curtain wall and the other exterior subassemblies were installed at the base of each corner supported by cantilevered concrete slabs. Figure 1(b) presents a plan view of the test specimen illustrating the locations of the rocking walls and exterior subassemblies. The curtain wall is denoted CW, while the CFS-framed subassemblies are denoted CFS 1, CFS 2, and CFS 3, respectively.

2.2. Test Program

The building test plan consists of 88 earthquake motions (a combination of unidirectional X or Y, bidirectional XY and tridirectional XYZ) that were applied with generally increasing intensities and include white noise between motions. Each earthquake record was amplitude scaled to achieve a target hazard level, which is correlated to its return period. Following table tuning, the test program began with 43-year motions at Motion

ID 13 (or MID13), then introduced 225-year motions at MID23, 475-year motions at MID32, 975-year motions at MID77, and risk-targeted maximum considered earthquake (MCE_R) at MID88. Additional details regarding the motion selection, scaling and final test protocol may be found in Wichman (2023). For conciseness, 22 critical motions have been utilized here to study the curtain walls performance. The list includes at least one iteration of each distinct record scaled to hazard level of 475 years or greater, all XYZ motions, and 2 sets of motions that included the full suite of X, Y, XY, and XYZ motions. Table 1 presents the 22 selected earthquake records along with their Motion ID, hazard levels, earthquake names and directionalities, peak table accelerations, and peak interstory drifts (ISDs) for the first two stories that the curtain wall spans (derived as described in Section 4.1).

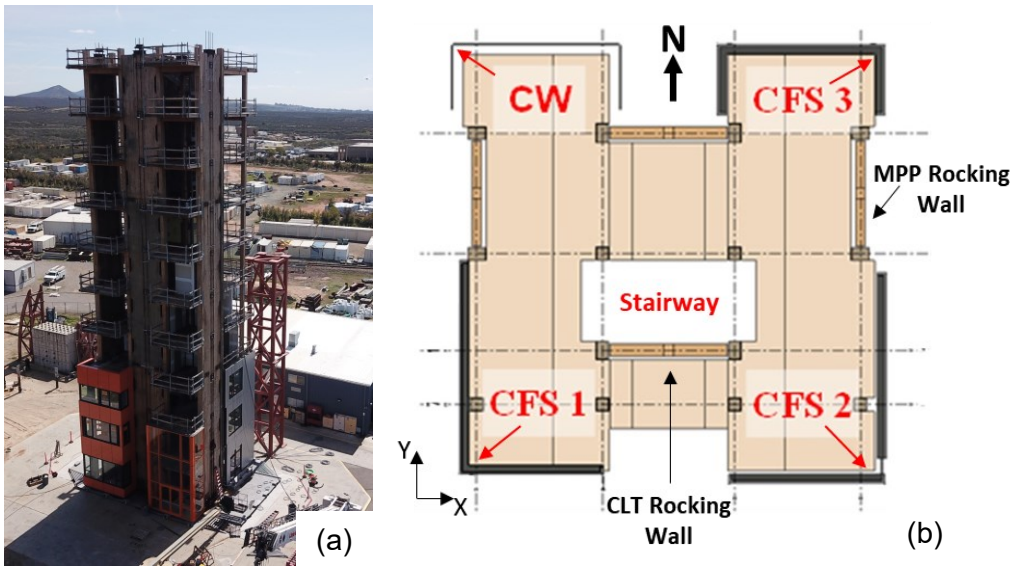

Figure 1. (a) Photo of the 10-story test specimen (view looking at CW, of the north-east corner) and (b) plan-view with the locations of the nonstructural exterior walls annotated

Table 1. Summary of the critical ground motions selected in this study

Motion ID	Hazard Level	Earthquake Name – Station – Direction	Peak Table Accelerations (g)			Peak ISD (%)			
						Story 1		Story 2	
			X	Y	Z	X	Y	X	Y
MID44	475	1994 Northridge – Compton-Castlegate – XYZ	0.36	0.26	0.19	0.36	0.37	0.48	0.43
MID46	475	1999 Chi-Chi – TCU075 – XY	0.47	0.27	0.02	0.42	0.43	0.63	0.59
MID56	43	1992 Ferndale – 1746 – XYZ	0.07	0.07	0.11	0.06	0.06	0.08	0.09
MID59	225	1992 Ferndale – 1746 – XY	0.20	0.26	0.01	0.23	0.25	0.28	0.18
MID62	225	2011 Tohoku – CHBH04 – XY	0.20	0.20	0.01	0.19	0.21	0.28	0.36
MID69	225	2004 Niigata – NIG023 – XYZ	0.24	0.34	0.08	0.17	0.20	0.24	0.32
MID70	475	1999 Chi-Chi – TCU075 – X	0.47	0.02	0.02	0.48	0.13	0.61	0.12
MID71	475	1999 Chi-Chi – TCU075 – Y	0.03	0.29	0.01	0.10	0.44	0.07	0.60
MID75	475	1992 Ferndale – 1746 – XYZ	0.31	0.39	0.42	0.32	0.40	0.48	0.38
MID76	475	2011 Tohoku – CHBH04 – X	0.34	0.02	0.01	0.25	0.08	0.33	0.08
MID77	975	1994 Northridge – Compton-Castlegate – X	0.53	0.03	0.02	0.63	0.13	0.73	0.14

MID78	975	1994 Northridge – Compton-Castlegate – Y	0.02	0.40	0.01	0.12	0.58	0.09	0.79
MID79	975	1994 Northridge – Compton-Castlegate – XY	0.52	0.40	0.02	0.68	0.62	0.77	0.79
MID81	475	1999 Chi-Chi – TCU075 – XYZ	0.46	0.26	0.33	0.45	0.43	0.59	0.60
MID82	975	2011 Tohoku – CHBH04 – X	0.50	0.03	0.01	0.53	0.12	0.70	0.13
MID86	975	1994 Northridge – Compton-Castlegate – XYZ	0.52	0.40	0.26	0.72	0.63	0.80	0.80
MID87	975	1992 Ferndale – 89486 – XYZ	0.45	0.49	0.42	0.45	0.50	0.50	0.54
MID88	MCE_R	1989 Loma Prieta – Freemont, Emerson Ct. – XYZ	0.53	0.73	0.18	0.44	0.79	0.57	0.87
MID90	MCE_R	1992 Ferndale – 89486 – XYZ	0.64	0.67	0.78	0.61	0.66	0.64	0.67
MID91	975	2003 Tokachi – HKD127 – X	0.37	0.02	0.02	1.03	0.25	1.14	0.22
MID92	975	1980 Victoria, Mexico – SAHOP Casa Flores – XYZ	0.18	0.52	0.32	0.76	0.67	0.87	0.72
MID93	MCE_R	2011 Tohoku – CHBH04 – X	0.70	0.03	0.02	0.90	0.16	1.09	0.15

3. Overview and Design of Curtain Wall System

3.1. Curtain Wall System

The curtain wall system was included in the test structure as a two-story exterior façade. This C-shaped, stick-built curtain wall enclosed the northwest corner of the building on the lower two levels as shown in Figure 2. Traditional curtain wall systems are framed with aluminum transoms and mullions—the horizontal and vertical framing members, respectively—and incorporate insulated glass units (IGUs) with two 6.35 mm (1/4”) lites (or glazing panels) separated by an insulating air cavity, typically resulting in an overall thickness of approximately 25 mm (1”). However, the 60-minute fire-rated curtain wall system in this test utilized stiffer S235JR steel mullions along with 27 mm (1-1/16”) thick multilayer-laminated glazing, which is comparable in thickness to the standard IGU. The glazing is composed of thin sheets of annealed glass between intumescent layers added for fire protection.

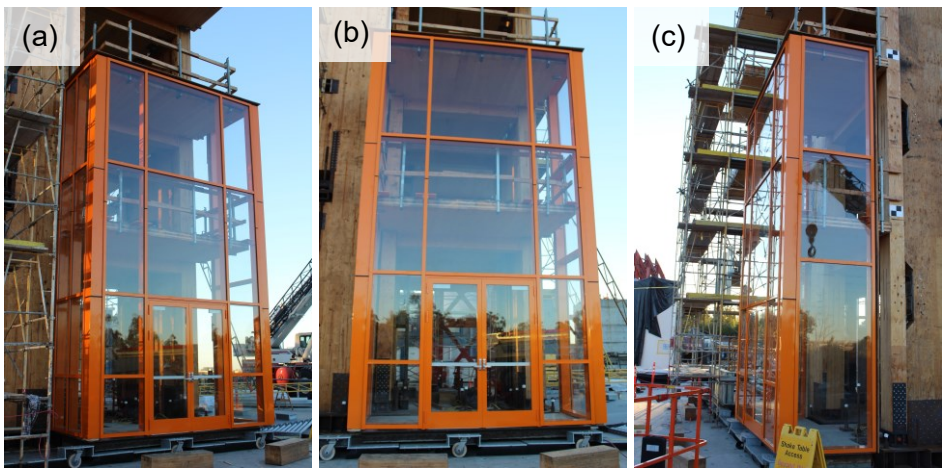

Figure 2: Views of the (a) east, (b) north, and (c) west faces of the curtain wall

The 2-story curtain wall stands 7.3 m (288”) from head to sill. The front wall is 4.3 m (170”) long, while the two side walls are 1.66 m (65”) long. The curtain wall subassembly incorporated glass lites that met the

specifications for maximum allowable glazing area on the front wall and the tallest allowable glazing on the west facing side wall, to test how the aspect ratio of the glazing panels affect the seismic performance. The glass lite with the maximum allowable area was 1995 mm by 2540 mm (79”x100”), while the tallest allowable glass lite was 1343 mm by 3000 mm (53”x120.5”).

The curtain wall subassembly was supported at the base of the structure on the steel ledger protruding from the edge of the concrete foundation slab using Nelson Weld Studs and slotted sill anchors as shown in Figure 3(a). Figures 3(b) and (c) illustrate how the framing of the curtain wall system was attached directly to the second and third floor diaphragms using vertically slotted wind-load and head anchors, respectively. The anchorage demands were calculated based on the design criteria as described in the following subsection.

Figure 3: (a) Slotted sill anchor at the foundation, (b) slotted windload anchors at 2nd floor diaphragm, and (c) slotted head anchors at 3rd floor diaphragm.

3.2. Curtain Wall Design Criteria

The demands of the curtain wall were calculated based on the 2018 IBC (2017) and ASCE 7-16 (2017) considering dead, wind, and seismic loading. The test specimen was classified as an Exposure C, Risk Category II, partially open building with a 3-second wind gust of 155 km/h (96 mph) and Mean Roof Height of 35 m (115’). Following ASCE 7-16 Section 30.5, the leeward wind direction controlled the design, and the wind pressure was constant over the height of the building. Thereby, the typical design wind pressure for the curtain wall was 1.36 kN/m^2 (28.6 psf) and the end zone design wind pressure was 2.51 kN/m^2 (52.5 psf).

The seismic demands on the curtain wall were obtained based on the performance-based design objective that the nonstructural components experience minimal damage at MCE$_R$ level ground motions. Therefore, ASCE 7-16 Eq. 13.3-1 was modified, aiming for the curtain wall to remain elastic under MCE$_R$ level ground motions. When calculating the total lateral seismic force F_p from ASCE 7-16 Eq. 13.3-1, the MCE$_R$ spectral coefficient at short periods S_{MS}—taken as 1.654—replaced S_{DS} and the R_p/I_p ratio was taken as 1.0 to design for elastic response. The component amplification factor a_p was taken as 1.0 for the curtain wall itself, but for the design of the connectors, a_p was taken as 1.25. The unit weight of the curtain wall system W_p was 0.79 kN/m^2 (16.5 psf), which includes the weight of the glass, framing and miscellaneous materials. Finally, the total lateral seismic force was found to be $0.94W_p$ (or 0.74 kN/m^2) for the curtain wall and $1.18W_p$ (or 0.93 kN/m^2) for the connections. Therefore, the connection design was controlled by out-of-plane wind loading.

4. Experimental Results

4.1. Building Response

The test structure was instrumented with accelerometers located at the approximate center of mass of each level to record the floor acceleration in the two horizontal directions, as well as the vertical direction. Due to the height of the building, displacement transducers could not be connected from a stationary structure to the test structure to directly measure story drifts above the 4th floor. Therefore, the story drifts were obtained by double integrating the recorded accelerations. Due to inherent noise in the acceleration signals, sensitivity to filtering parameters, and potential orientation issues, there is uncertainty in the accuracy of the obtained drifts. The peak ISDs in the global X and Y directions for each of the selected motions are presented in Figure 4. The peak ISD profile illustrates that the curtain wall—located at the first two stories—generally experienced lower ISD demands than the upper stories.

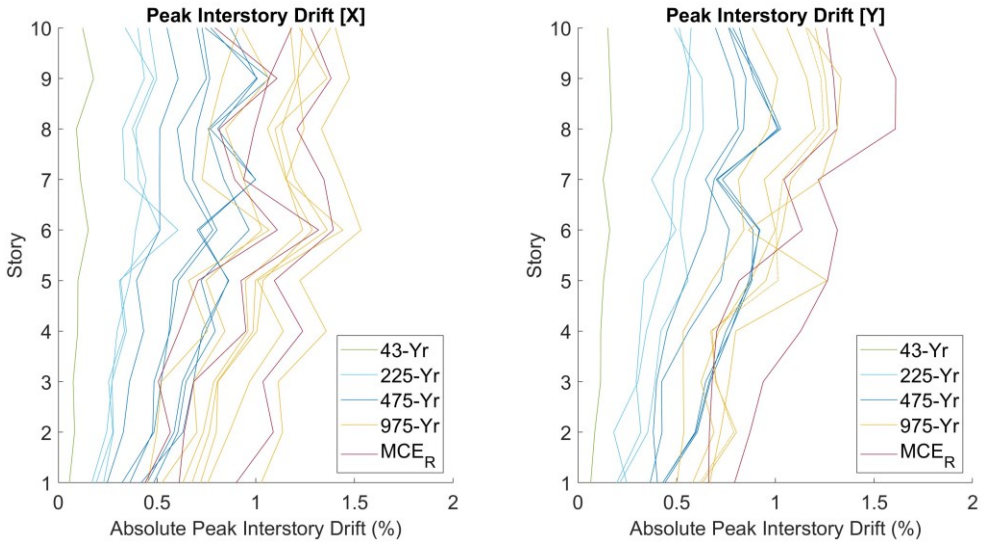

Figure 4: Absolute peak interstory drift at each story in the X- and Y-directions for each of the selected ground motions

The peak floor accelerations (PFAs) are presented in Figure 5. Similar to the peak ISD profile, the PFA generally increases at higher levels. Thus, the acceleration demands applied to the curtain wall are lower compared to the components at higher levels. It is important to note that in an actual building, the curtain wall system would span the entire height of the building and would experience higher drift and acceleration demands than what was experienced in this test program.

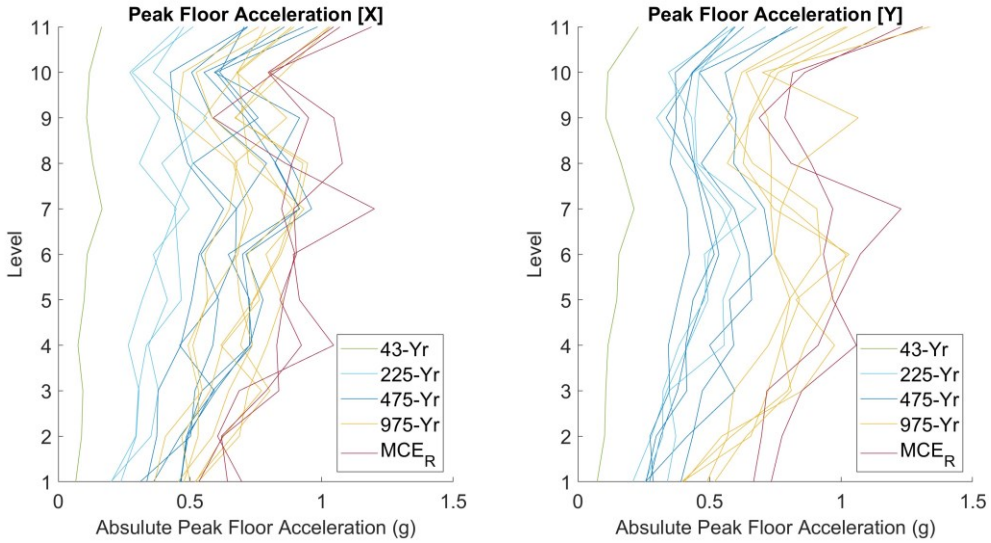

Figure 5: Absolute peak floor acceleration at each level in the X-, Y-, and Z-directions for each of the selected ground motions

Triaxial accelerometers were installed on each of the concrete foundation slabs to monitor the vibrations as they represent direct inputs to the exterior façade subassemblies, particularly in the vertical direction. Figure 6 presents the acceleration histories recorded at the shake table center of mass and concrete slab located on the northwest corner of the building, which supports the curtain wall system, for the MID69 test. These acceleration histories show that the table and concrete slab accelerations are nearly identical in the X- and Y-directions. However, vertical acceleration is significantly amplified on the concrete slab compared to the shake table. Figure 7 presents vertical acceleration amplification factor (concrete slab acceleration to table acceleration) versus vertical table acceleration. This figure illustrates that the average vertical acceleration input to the curtain wall is twice the table acceleration.

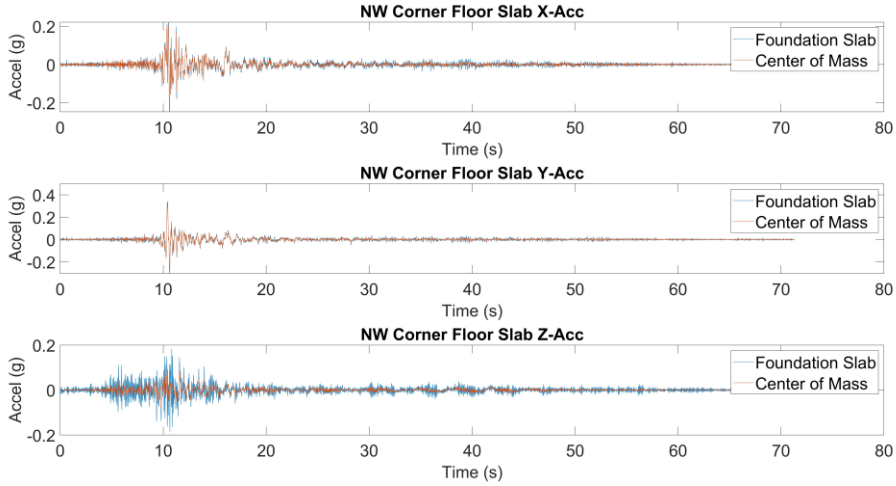

Figure 6: Acceleration history of the table (top of platen) and edge of the northwest cantilevered concrete slab during MID69 – 225 Niigata XYZ

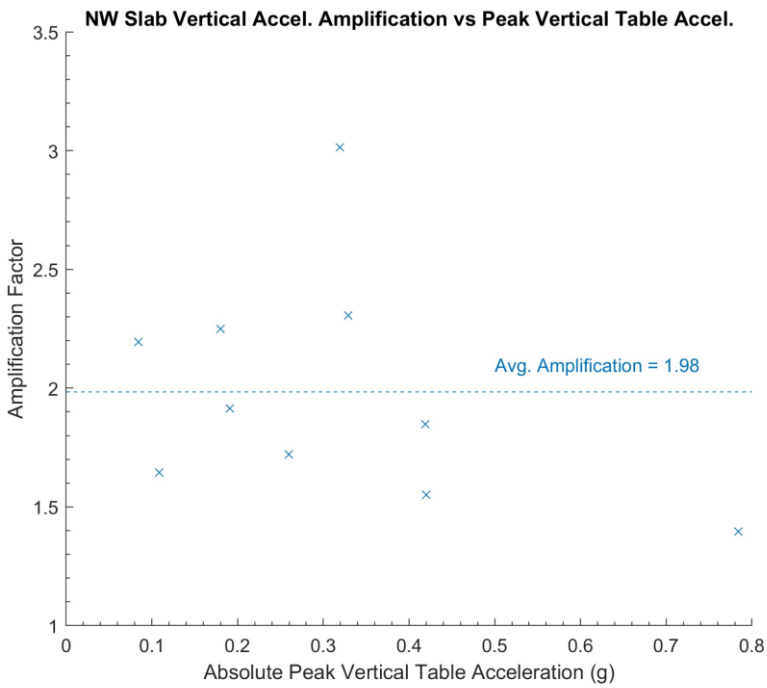

Figure 7: Vertical acceleration amplification of the cantilevered concrete slab versus peak vertical ground acceleration at the table platen

4.2. Physical Observations

The curtain wall system performed well throughout the duration of the test program. Some minor damage was observed, but none that was life-threatening or would affect the serviceability of the building. It is important to note that these damages occurred after many strong motions, much more than an actual building would experience. The results of the physical inspection of the test structure are as follows:

- During construction of the curtain wall, a 12.7 mm (½") plywood cover was installed at the head of the curtain wall and fastened to the third-floor slab to serve as an artificial top-of-wall and provide a fire-resistant, air- and water-proof seal to the system. Prior to testing, warping of the plywood cover was observed due to changes in the weather conditions. After MID41, three of the screws securing the plywood panel cover at the head of the curtain wall had failed. Further inspection indicated that after

MID46, the seal—which was being held together only by the caulking after the fasteners failed—had completely failed.

- Prior to testing, the corners of the glass lites were spray-painted to indicate movement of the glass within the glazing pocket during testing as shown in Figure 8(a). Figure 8(b) shows that initially, following lower intensity motions (<225-year return period), movement was apparent during shaking as the paint exhibited some separation but had returned to its initial position. At higher intensities (>475-year return period), it was apparent that the glass lites had begun to shift slightly. After MID88, a significant shift in the glass panel at the top west corner on Level 2 was observed; the tape around the glass became exposed as illustrated in Figure 8(c). In the subsequent ground motions, other glass lites shifted more noticeably from their original positions.
- The slotted anchors connecting the vertical mullions to the floor slabs were intended to accommodate vertical movement of the curtain wall relative to the floor slabs. The bolts in the slots of the wind load anchors at Level 2 were spray-painted to identify movement across the slotted connection. Observations revealed that approximately 1 cm of residual movement had occurred, indicating that the connection accommodated the vertical movement.
- During testing, the curtain wall doors were visibly opening and closing. By the end of the test program, after MID100, one of the doors would not close properly because the door latch rod was permanently bent as shown in Figure 9(a) and (b). Figure 9(c) illustrates the widened door latch insertion holes, which may have been caused by vertical shaking. The damage to the door latch mechanism compromises the fire-resistance of the door system within the curtain wall, as door closure is essential to preventing fire-spread.

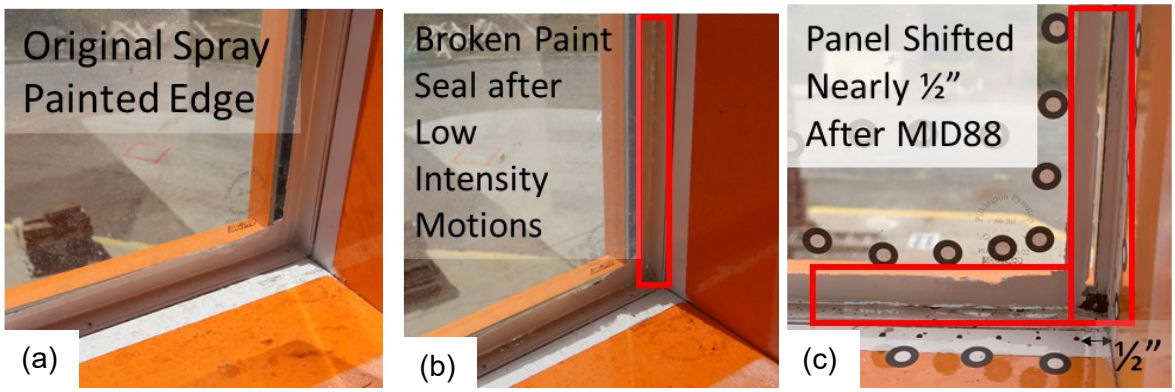

Figure 8: Spray painted edge of the top west panel on 2nd story (a) before testing, (b) after low intensity motions, and (c) after MID88 – MCE_R Loma Prieta XYZ

Figure 9: (a) Door latch mechanism preventing closure and (b) close up of damaged door latch, with (c) apparent damage to the door latch mechanisms' openings at end of testing

4.3. Curtain Wall Response

The curtain wall was instrumented with 12 accelerometers and 16 linear potentiometers at critical locations to monitor its response. Figure 10 presents the locations and naming conventions for the sensors and instrumented glass lites. Component accelerations were measured in the X, Y, and Z directions at each location. Two sets of accelerometers were located on the transoms above and below the middle north panel (MNP). Another set of accelerometers was located on the transom above the bottom west panel (BWP), while the other set of accelerometers was located on the corner mullion directly above the 2nd floor diaphragm. The locations of the accelerometers were selected to observe the component amplification effects above and below the largest panel (MNP TT and MNP BT, respectively), above the tallest panel (BWP), and at the 2nd floor slab (Corner Mullion).

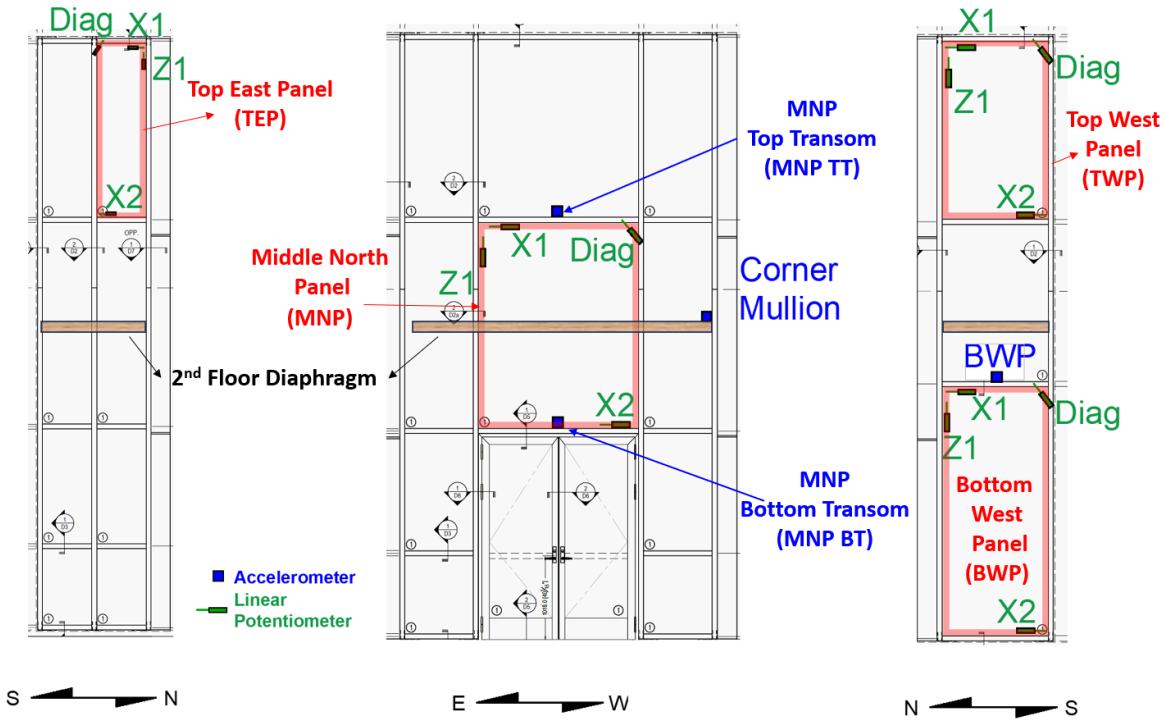

Figure 10: Locations and nomenclature of the curtain wall instrumentation

The effect of the in-plane, out-of-plane, and vertical PFAs on the component amplification factor, or ratio of the peak component acceleration (PCA) to the PFAs at the various locations are presented in Figure 11. The input PFA was taken from the corresponding level that the sensor was installed, except the vertical floor accelerations were taken from the concrete foundation because of the amplification effect. The component amplification factor does not appear to be affected by the magnitude of the PFA. Likewise, component amplifications in-plane and out-of-plane are similar, except for MNP TT, which experiences increased component amplification out-of-plane. The component amplification factor generally ranges between 1.1 and 2.5, while up to 3.5 for MPT TT out-of-plane. In the Z-direction, the PCA/PFA amplitude ranges between 1.0 and 2.5 above 0.2g, except for BWP. The component amplification is higher at vertical PFAs less than 0.2g. The vertical component amplification in the BWP is much less than the other accelerometer locations. In fact, it is the only location where acceleration was attenuated, as the component amplification is less than 1.0 for many of the ground motions.

Linear potentiometers, as mentioned above, were intended to measure the movement of the glass panels within the glazing pocket relative to the curtain wall framing. The authors could not find a precedent for using displacement sensors to measure glass movement in prior experiments. Each of the instrumented panels included linear potentiometers to measure: the relative horizontal displacement between the glass and the framing at the top and bottom of the panels (X1 and X2, respectively), the relative vertical displacement of the panels (Z1), and the change in length of the transom-to-mullion connection (Diag). The change in length of the diagonal linear potentiometers can be used to determine the rotation at the transom-mullion connections.

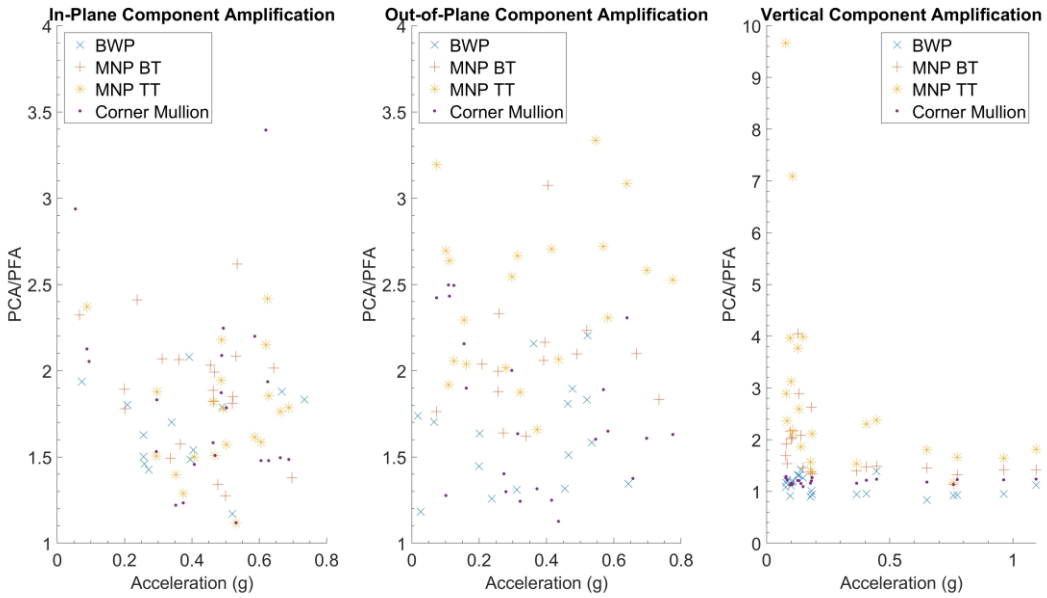

Figure 11: Component amplification factor (absolute peak component acceleration / peak floor acceleration) PCA/PFA versus PFA

The displacement histories of the linear potentiometers instrumented on the Middle North Panel (MNP) during MID93 are presented in Figure 12. Larger relative movements were observed at X1 and Z1 than at X2, with small displacements observed in the diagonal linear potentiometer. The difference between the X1 and X2 values indicates that the glass panel was subjected to both rotation and translation within the framing, and the data measuring the framing may give insight to the panel movement in terms of its drift accommodation mechanisms. Figure 13 shows the extent of the panel movement from its initial position to one of its peak displacements during MID93.

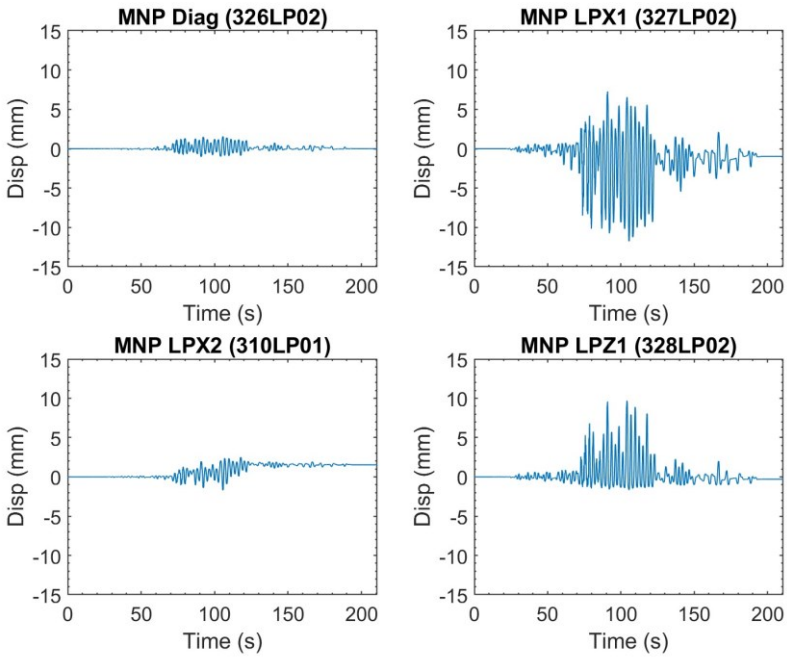

Figure 12: Middle North Panel (MNP) linear potentiometer time histories during MID93 – MCE_R Tohoku X

Figure 13: Panel movement during MID93 – MCE$_R$ Tohoku X at (a) time = 0 sec and (b) time = 108 sec

Figure 14 presents the relative panel displacement within the framing for different panel locations versus the in-plane peak ISD for each of the selected motions, excluding out-of-plane only motions. For instance, the in-plane drift considered for the MNP was in the global X direction and the Y-only motions were excluded. The relationship illustrates that the peak panel displacements essentially vary linearly with the in-plane peak ISD. The MNP is the only panel to experience larger X1 displacements than Z1 displacements, likely due to the larger aspect ratio (width-to-height) compared to the other panels. The panels with larger aspect ratios were noted to experience larger vertical displacements than the panels with smaller aspect ratios.

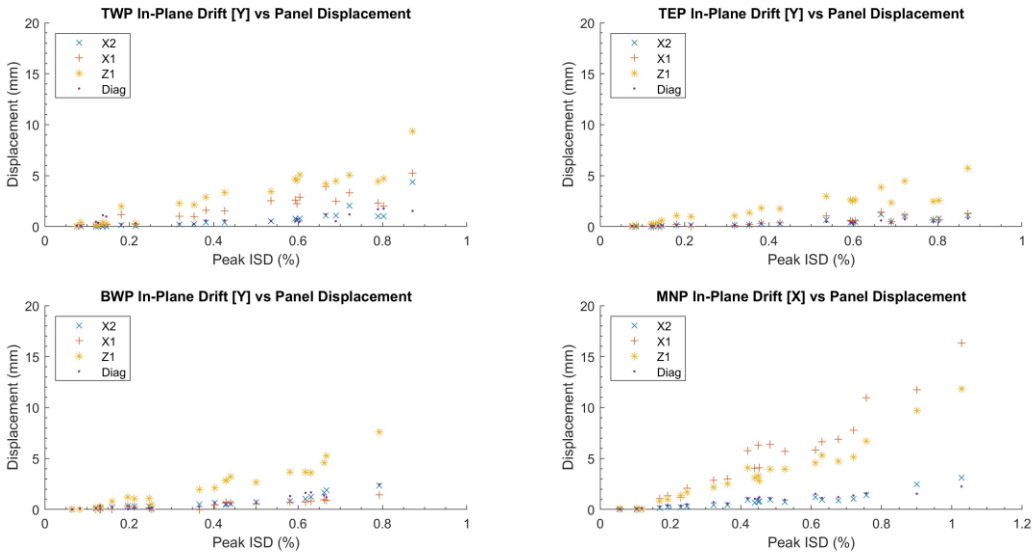

Figure 14: Peak ISD vs panels' relative displacement

5. Conclusions

A two-story, stick-built curtain wall system was incorporated as part a full-scale building shake table test. The key findings are as follows:

- The cantilevered foundation slab supporting the curtain wall caused the vertical input acceleration to be amplified 2-3 times the table input acceleration. The vertical slab accelerations represented the input acceleration for the curtain wall system.
- The effect of the in-plane, out-of-plane, and vertical PFAs on the component amplification factor at various locations were observed. In-plane and out-of-plane component amplification ranged from 1.1 to 3.5, while the top transom of the middle north panel sustained a higher component amplification in the out-of-plane direction than in-plane, likely due to its location between the second and third floor diaphragms.

- Linear potentiometers were installed to measure the movement of the glass panels within the glazing pocket relative to the curtain wall framing. The relative movement of the glazing panels within the frame displays a linear relationship with the in-plane drift.
- The curtain wall system experienced only minor damage that would not affect a building's serviceability. The most notable damage observed was a cumulative shifting of the top west panel such that one corner was at risk of dislodging from the glazing pocket. However, the panel was contained in the glazing pocket around the other edges, so there was no imminent risk of the entire panel dislodging. Other damage observations include failure of the door latch mechanism and failure of the weatherproof and fire-resistant seal at the head of the system. This damage may have compromised the fire-resistance and weathertightness of certain locations on the curtain wall, and some repairs may be necessary in an actual structure. It is important to note that this damage occurred after many strong motions, much more than an actual building would experience.

6. Acknowledgements

The structural system scope of NHERI TallWood Project is sponsored by NSF Grants No. 1635227, 1634628, 1634204. The use and operation of NHERI shake table facility is supported by NSF through Grant No.1520904. The nonstructural component scope of this project is sponsored by NSF Grant No. CMMI-1635363, USFS Grant No. 19-DG-11046000-16, Softwood Lumber Board, Computers and Structures Inc, the GAANN Fellowship Program at UNR, and industry sponsors. Materials and in-kind support for the curtain wall subassembly discussed in this paper are provided by Technical Glass Products, a subsidiary of Allegion. The authors are indebted to the many contributors that made this project possible. Any opinion, findings, and conclusions or recommendations expressed in this material are those of the authors and do not necessarily reflect the views of the National Science Foundation.

7. References

American Architectural Manufacturers Association (2018). *Recommended Dynamic Test Method for Determining the Seismic Drift Causing Glass Fallout from Window Wall, Curtain Wall and Storefront Systems*, Publication No. AAMA 501.6-18.

American Society of Civil Engineers (2017). *ASCE/SEI 7-16: Minimum design loads and associated criteria for buildings and other structures*. American Society of Civil Engineers.

Behr, R.A., Belarbi, A. and Culp, J.H. (1995). Dynamic racking tests of curtain wall glass elements with in-plane and out-of-plane motions. *Earthquake engineering & structural dynamics*, *24*(1), pp.1-14.

Behr, R.A. (1998). Seismic performance of architectural glass in mid-rise curtain wall. *Journal of architectural engineering*, *4*(3), pp.94-98.

Busch, A. (2023). "Design and Construction of Tall Mass Timber Buildings with Resilient Post-Tensioned Mass Timber Rocking Walls." Ph.D Thesis, Colorado School of Mines, Golden, CO.

Ganey, R., Berman, J., Akbas, T., Loftus, S., Daniel Dolan, J., Sause, R., Ricles, J., Pei, S., Lindt, J.V.D. and Blomgren, H.E. (2017). Experimental investigation of self-centering cross-laminated timber walls. *Journal of Structural Engineering*, *143*(10), p.04017135.

Memari, A.M., Shirazi, A., Kremer, P.A. and Behr, R.A. (2011). Development of finite-element modeling approach for lateral load analysis of dry-glazed curtain walls. *Journal of architectural engineering*, *17*(1), pp.24-33.

International Code Council (2017). *2018 International Building Code*. International Code Council, Inc. Falls Church, Va

Pei, S., van de Lindt, J.W., Barbosa, A.R., Berman, J.W., McDonnell, E., Daniel Dolan, J., Blomgren, H.E., Zimmerman, R.B., Huang, D. and Wichman, S. (2019). Experimental seismic response of a resilient 2-story mass-timber building with post-tensioned rocking walls. *Journal of Structural Engineering*, *145*(11), p.04019120.

Wichman, S. (2023). "Seismic Behavior of Tall Rocking Mass Timber Walls." Ph.D. Thesis, University of Washington, Seattle, WA.